Hindawi
Advances in Materials Science and Engineering
Volume 2018, Article ID 4026127, 6 pages
https://doi.org/10.1155/2018/4026127

Research Article

Influence of Pb Dosage on Immobilization Characteristics of Different Types of Alkali-Activated Mixtures and Mortars

Jan Koplík, Jaromír Pořízka, Lukáš Kalina, Jiří Másilko, and Matěj Březina

Faculty of Chemistry, Materials Research Centre, Brno University of Technology, Purkyňova 118, 612 00 Brno, Czech Republic

Correspondence should be addressed to Jan Koplík; koplik@fch.vutbr.cz

Received 9 June 2017; Revised 31 October 2017; Accepted 28 November 2017; Published 11 January 2018

Academic Editor: Kedsarin Pimraksa

Alkali-activated matrices are suitable materials for the immobilization of hazardous materials such as heavy metals. This paper is focused on the comparison of immobilization characteristics of various inorganic composite materials based on blast furnace slag and on the influence of various dosages of the heavy metal Pb on the mechanical properties and fixation ability of prepared matrices. Blast furnace slag (BFS), fly ash, and standard sand were used as raw materials, and sodium water glass was used as an alkaline activator. $Pb(NO_3)_2$ served as a source of heavy metal and was added in various dosages in solid state or as aqueous solution. The immobilization characteristics were determined by leaching tests, and the content of Pb in the eluate was measured by inductively coupled plasma optical emission spectroscopy (ICP-OES). The microstructure of matrices and distribution of Pb within the matrix were determined by scanning electron microscopy (SEM) equipped with energy dispersive X-ray spectroscopy (EDS). Increasing the dosage of the heavy metal had negative impacts on the mechanical properties of prepared matrices. The leaching tests confirmed the ability of alkali-activated materials to immobilize heavy metals. With increasing addition of Pb, its content in eluates increased.

1. Introduction

Heavy metals such as Pb belong to hazardous materials, which are harmful to the human beings. Lead is highly toxic element, which attacks mainly the nervous system. Lead exposure mostly occurs through the ingestion of contaminated water or food. Therefore, it is important to prevent its leakage into the environment by stabilization or solidification of waste materials before their deposition into the landfill [1]. A possible way on how to immobilize heavy metals is using alkali-activated materials (AAMs). AAMs present a broad range of materials (geopolymers, activated blast furnace slag, etc.), but all of them are activated by high pH during their preparation. The AAMs can be divided into two big groups: high-calcium alkali-activated materials (HCAAMs) and low-calcium alkali-activated materials (LCAAMs). HCAAMs are represented mainly by activated BFS, and LCAAMs are represented mainly by activated fly ash or metakaolin. The structure of HCAAMs consists of the C-A-S-H gel as a major hydration product. This gel has a similar structure as the C-S-H gel in hydrated ordinary Portland cement and is made up of tetrahedrally coordinated silicate chains, where aluminium is located in the bridging position instead of silicon. The structure and composition of the C-A-S-H gel depend on the nature and concentration of the used activator. AFm-type phases (NaOH-activated binders), hydrotalcite (BFS with high content of MgO), and zeolites (binders with high content of Al_2O_3) are usually formed as secondary hydration products [2–4].

Heavy metals can be immobilized by two types of fixation–physical and chemical. Mostly, both types of immobilization occur together. Physical fixation is linked with mechanical properties and porosity of the matrix. Chemical fixation means that there is a chemical bond between the heavy metal and the matrix. Heavy metals can be inhibited by transformation into a less soluble form as well. After alkali activation, the heavy metals usually occur in the form of silicate or hydroxide [5–7]. The

Table 1: Particle size distribution of raw materials.

	x (10%) μm	x (50%) μm	x (90%) μm	x (99%) μm
BFS	0.88	10.73	33.97	59.57
Fly ash	4.18	44.56	236.89	486.20

Table 2: The nomenclature of samples.

Mixture	Mixture name
BFS; 1% Pb added as solid	S1
BFS; 2.5% Pb added as solid	S2
BFS; 5% Pb added as solid	S5
BFS + sand; 1% Pb added as solid	M1
BFS + sand; 2.5% Pb added as solid	M2
BFS + sand; 5% Pb added as solid	M5
BFS + fly ash; 1% Pb added as solid	P1
BFS + fly ash; 2.5% Pb added as solid	P2
BFS + fly ash; 5% Pb added as solid	P5
BFS; 1% Pb added as liquid	SR1
BFS; 2.5% Pb added as liquid	SR2
BFS + sand; 1% Pb added as liquid	MR1
BFS + sand; 2.5% Pb added as liquid	MR2
BFS + fly ash; 1% Pb added as liquid	PR1
BFS + fly ash; 2.5% Pb added as liquid	PR2

Table 3: The mixture design of prepared matrices.

	BFS matrices	Matrices with sand	Matrices with fly ash
BFS	100 wt.%	25 wt.%	50 wt.%
Fly ash	—	—	50 wt.%
Sand	—	75 wt.%	—
Activator/binder	8%	8%	8%
Water/binder	0.33	0.42	0.33

immobilization of heavy metals within AAMs can be influenced by various factors, such as the composition of the matrix, the type of alkaline activator, the immobilized heavy metal, and the leaching medium [8, 9]. Previous researches proved that Pb reached high efficiency of immobilization in AAMs, but there is only little information about the influence of Pb dosage on immobilization characteristics of AAMs [10–13].

The aim of this work was to compare the ability of three different alkali-activated matrices based on BFS to immobilize Pb within their structure. The influence of different Pb dosages on the immobilization efficiency was also investigated.

2. Materials and Methods

2.1. Materials, Sample Preparation, and Leaching Tests. BFS and high-temperature fly ash were used as raw materials. The particle size distribution of both raw materials is listed in Table 1. Liquid sodium silicate with the SiO_2/Na_2O ratio of 1.85 served as an alkaline activator. As fine aggregates, three different fractions of siliceous Czech standard sand complying with ČSN EN 196-1 were used (the mass ratio of the fractions was 1 : 1 : 1). Pb was used in the form of $Pb(NO_3)_2$.

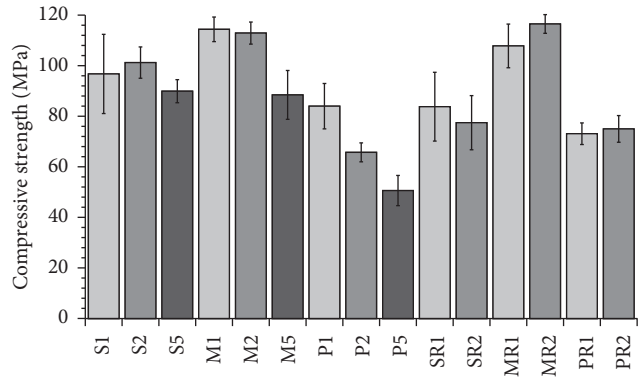

Figure 1: Compressive strength of prepared matrices (28 days).

Three types of matrices were prepared. The first one was based only on BFS. In the second one, 50 wt.% of BFS was replaced by fly ash. And the third one consisted of BFS and standard sand. The sample nomenclature and the mixture designs are listed in Tables 2 and 3, respectively. Pb was added in the dosages of 1, 2.5, and 5 wt.% to binder mass and was added in two ways: as a solution and as a solid. In both cases, the water-to-binder ratios were the same.

The whole mixing procedure took four minutes. In the beginning, all materials without aggregates were put together and sand, if needed, was added after 30 s of mixing. The samples were cast in steel molds measuring $20 \times 20 \times 100$ mm. All analyses were performed after 28 days of moist curing (98% relative humidity) at laboratory temperature ($23 \pm 2^{\circ}$C).

The leaching tests were based on ČSN EN 12457-4. The demineralized water served as leaching agent. The solid/liquid ratio was 1 : 10, and the mixture was agitated for 24 hours. After the leaching time ended, the mixture was filtered by a membrane filter with the pore size of 0.45 μm, and the concentration of Pb in solution was determined by ICP-OES.

2.2. Methods. The compressive strength was measured according to the ČSN EN 196-1 using Betonsystem Desttest 3310. To determine the porosity, prepared matrices were investigated by mercury intrusion porosimetry using Quantachrome instrument PoreMaster 33. The surface tension of mercury was 480 mN/m, and the contact angle was 140° based on the recommendation. The pore sizes were determined in the range from over 170 μm to 0.0064 μm. The ICP-OES data were obtained using Horiba Jobin Yvon Ultima II Spectrometer. The parameters of measurement were as follows: RF power, 1350 W; gas, argon; plasma gas, 13 L·min^{-1}; auxiliary gas, 0.1 L·min^{-1}; nebuliser gas, 0.85 L·min^{-1}; plasma view, radial; nebuliser, Meinhard; and nebuliser pressure, 3 bar. The scanning electron microscopy (SEM) and the energy dispersive X-ray spectroscopy (EDS)

Table 4: Compressive strength of prepared matrices (7 days).

Mixture	S1	S2	S5	M1	M2	M5	P1	P2
MPa	62.3	61.8	58.3	75.0	74.8	59.7	56.7	49.7
Mixture	P5	SR1	SR2	MR1	MR2	PR1	PR2	—
MPa	40.1	55.4	53.2	70.5	76.3	50.3	52.7	—

Table 5: The porosity of matrices.

Total intruded volume (cm^3/g)	P1	P5	PR1	M1	M5	MR1	S1	S5	SR1
	0.130	1.312	0.117	0.034	0.050	0.036	0.022	0.035	0.023

analyses were performed using Zeiss EVO LS 10 equipped with an Oxford X-Max 80 mm^2 detector in the backscattering mode. The working distance for all samples was 12 mm and the accelerate voltage was 30 kV. All samples were sputtered by carbon to obtain good surface conductivity.

3. Results and Discussion

3.1. Compressive Strength. The compressive strength of prepared matrices is shown in Figure 1 and Table 4. Following the results, the type of matrix had the highest influence on the compressive strength. The highest values had the matrix with aggregates, and the lowest values reached the matrix with fly ash. The results correspond with the findings in literature that, by replacing BFS with fly ash, the compressive strength decreases [2]. No clear behavior correlation was observed between the Pb dosage amount and mechanical properties. Increasing the dosage of Pb from 1 up to 2.5 wt.% led, in some cases, to the compressive strength increase and in some cases to the strength decrease. The addition of 5 wt.% of Pb caused the decrease of compressive strength in all types of matrices.

3.2. Porosity. The porosity of the prepared materials depended mainly on the type of the matrix. The total porosity of chosen samples is listed in Table 5. The matrix with fly ash showed the highest porosity. High-temperature fly ash consists of spherical particles, which can be filled in with similar smaller particles or can be hollow. Hence, partially reacted fly ash particles increased the porosity. The lowest porosity was observed in the matrix based on BFS. It is due to a very compact microstructure of this matrix, which was confirmed by SEM analysis (Figure 2). The dosage of Pb influenced the porosity of matrices too. The total porosity of matrices increased with increasing Pb content. As can be seen in Figure 3, around the areas, where Pb was cummulated, the matrix was not compact and the cracks and pores were formed. This caused the increase in porosity. The state of Pb addition—liquid/solid—did not affect the porosity.

3.3. Leaching Tests. To determine the efficiency of Pb immobilization, the leaching test based on ČSN EN 12457-4

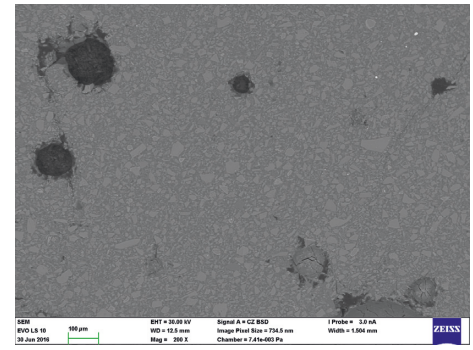

Figure 2: The microstructure of SR2 matrix.

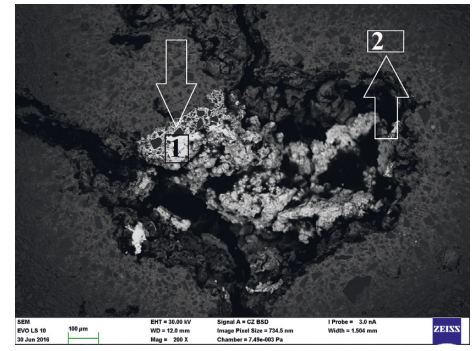

Figure 3: The microstructure of S2 matrix.

was performed. This test serves to determine whether the material is suitable for landfilling and whether it does not represent any hazard for the environment. Figure 4 shows the concentration of Pb in eluates from the prepared matrices. The immobilization of Pb in all matrices was very high and reached up to 99%. The results correspond with previous research and correlate with the total porosity of the matrices [11]. The highest Pb release occurred from matrices with fly ash, which also had the highest porosity and the lowest mechanical properties. The dosage of Pb had the influence on immobilization too. With increasing Pb addition, the content of Pb released into the leaching medium increased as well. It should be taken into consideration that when the Pb addition rose five times, the release increased only maximally three times. The efficiency of Pb immobilization was better with higher dosages of Pb.

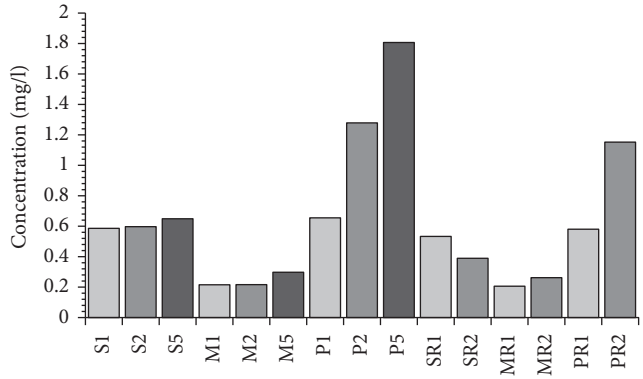

Figure 4: Concentration of Pb in eluates from matrices.

Table 6: The pH of eluates from matrices.

Mixture	S1	S2	S5	M1	M2	M5	P1	P2
pH	11.92	11.89	11.77	11.32	11.29	11.15	11.63	11.60
Mixture	P5	SR1	SR2	MR1	MR2	PR1	PR2	—
pH	11.51	11.89	11.88	11.31	11.31	11.63	11.58	—

Table 7: EDS analysis of S2 matrix.

					Area 1						
Element	O	Na	Mg	Al	Si	Ca	Pb	—	—	—	—
Atomic (%)	57.85	3.29	0.76	0.95	12.32	1.64	23.20	—	—	—	—
					Area 2						
Element	O	Na	Mg	Al	Si	Ca	Pb	S	K	Ti	Mn
Atomic (%)	58.13	4.62	3.93	3.00	15.23	12.80	0.97	0.88	0.19	0.07	0.18

Table 8: EDS analysis of P2 matrix.

					Area 3					
Element	O	Si	Ca	Al	Pb	—	—	—	—	—
Atomic (%)	81.61	3.95	3.61	1.03	9.79	—	—	—	—	—
					Area 4					
Element	O	Si	Ca	Al	Pb	Na	Mg	K	Ti	Fe
Atomic (%)	59.10	18.91	5.96	7.57	0.12	4.89	1.86	0.57	0.30	0.72

The pH of eluates is listed in Table 6. The matrices with sand reached the lowest pH, because they contained the smallest amount of the binder. The presence of fly ash led to the decrease of pH. The highest dosage of Pb (5 wt.%) caused the decrease of pH as well.

3.4. SEM. The SEM analysis showed three different microstructures depending on the type of matrix. The samples S2, P2, M2, and SR2 were investigated. The matrix based on BFS had a compact structure with unreacted particles of BFS and hydration products between them (Figure 3, Area 2; Table 7). A similar structure was observed in the matrix containing fly ash, but moreover, unreacted particles of fly ash were identified. The addition of fly ash led to the increase in the content of Si and Al and the decrease in the content of Ca (Table 8). A quite different microstructure occurred in the matrix with aggregates. The unreacted aggregates filled the major area of the sample and in between them there was the matrix with the same composition as observed in the S2 sample (Figure 5, Table 9, and Area 6). The aggregates were composed of quartz (Table 9 and Area 7).

When Pb was added as a solid, it behaved in the same manner in all types of matrices. Pb was cumulated in pores and formed specific structures (Figures 3, 5, and 6). These structures consisted mainly of Pb and O. It can be assumed that Pb transformed into its insoluble salt $Pb(OH)_2$ after the alkali activation. These findings correspond to previous research [14]. Minor amount of Pb was dispersed throughout the matrix. A quite different situation came up with the addition of Pb as a solution. Pb was dispersed

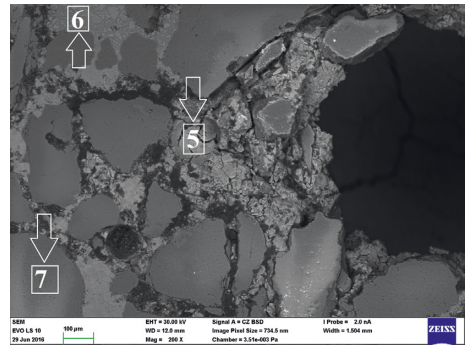

Figure 5: The microstructure of M2 matrix.

Table 9: EDS analysis of M2 matrix.

					Area 5						
Element	O	Si	Ca	Pb	—	—	—	—	—	—	—
Atomic (%)	73.26	7.61	5.21	13.92	—	—	—	—	—	—	—
					Area 6						
Element	O	Si	Ca	Pb	Na	Mg	Al	S	K	Ti	Mn
Atomic (%)	59.02	15.38	12.87	0.14	3.93	4.17	3.52	0.44	0.21	0.13	0.19
					Area 7						
Element	O	Si	—	—	—	—	—	—	—	—	—
Atomic (%)	63.65	36.35	—	—	—	—	—	—	—	—	—

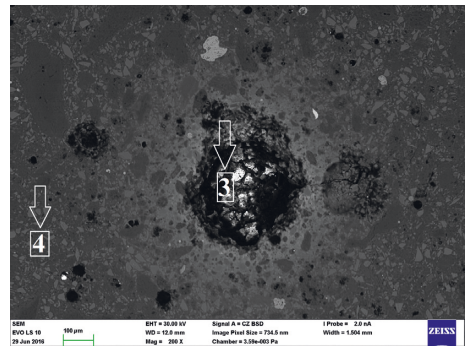

Figure 6: The microstructure of P2 matrix.

Table 10: EDS mapping of SR2 matrix.

Element	O	Si	Ca	Al	Pb	Na	Mg	K	Ti	Mn
Atomic (%)	58.96	15.39	13.06	3.08	0.27	4.65	3.86	0.18	0.07	0.15

equally throughout the matrix and did not create any specific structures (Figure 2, Table 10).

4. Conclusions

The immobilization of Pb in three different matrices was investigated. All matrices showed good ability to immobilize Pb. The increase in the Pb dosage led to the increase of Pb concentration in eluates, but the immobilization efficiency remained up to 99% in all cases. After the alkali activation, Pb formed its insoluble salt Pb $(OH)_2$. Both the compressive strength and the porosity were influenced by the Pb dosage. The decrease of mechanical properties after the addition of higher Pb dosage (5 wt.%) was observed. The concentration of Pb in eluates correlated with the porosity: when the porosity was higher, more Pb was released in eluates. It can be assumed that Pb was fixed by physical fixation, which was linked with the mechanical properties of matrices. Pb was also well immobilized, thanks to the formation of its insoluble

salt. There was a difference in Pb behavior when added either as a solid or as a solution. In the case of solution, Pb was dispersed throughout the matrix equally, but when added as a solid, it formed specific structures, which cumulated in pores.

Conflicts of Interest

The authors declare that there are no conflicts of interest regarding the publication of this paper.

Acknowledgments

This outcome has been achieved with the financial support by the project Materials Research Centre at FCH BUT-Sustainability and Development (REG LO1211), National Programme for Sustainability I (Ministry of Education, Youth and Sports), and "Development of shrinkage reducing agents designed for alkali activated systems" (GA17-03670S, Czech Science Foundation).

References

[1] J. M. Stellman, *Encyclopaedia of Occupational Health and Safety*, International Labour Office, Geneva, Switzerland, 4th edition, 1998.

[2] J. L. Provis and J. S. J. van Deventer, *Alkali Activated Materials: State-of-the-Art Report*, Springer, Dorderecht, Netherlands, 2014.

[3] L. Chao, S. Henghu, and L. Longtu, "A review: the comparison between alkali-activated slag (Si + Ca) and metakaolin (Si + Al) cements," *Cement and Concrete Research*, vol. 40, no. 9, pp. 1341–1349, 2010.

[4] F. Puertas, M. Palacios, H. Manzano, J. S. Dolado, A. Rico, and J. Rodríguez, "A model for the C-A-S-H gel formed in alkali-activated slag cements," *Journal of the European Ceramic Society*, vol. 31, no. 12, pp. 2043–2056, 2011.

[5] J. G. S. van Jaarsveld, J. S. J. van Deventer, and L. Lorenzen, "Factor affecting the immobilization of metals in geopolymerized fly ash," *Metallurgical and Materials Transactions B*, vol. 29, no. 1, pp. 283–291, 1998.

[6] J. W. Phair and J. S. J. van Deventer, "Effect of silicate activator pH on the leaching and material characteristic of waste-based inorganic polymer," *Minerals Engineering*, vol. 14, no. 3, pp. 289–304, 2001.

[7] A. Palomo and M. Palacios, "Alkali-activated cementious materials: alternative matrices for the immobilisation of hazardous wastes part II. Stabilisation of chromium and lead," *Cement and Concrete Research*, vol. 33, no. 2, pp. 289–295, 2003.

[8] J. W. Phair, J. S. J. van Deventer, and J. D. Smith, "Effect of Al source and alkali activation on Pb and Cu immobilisation in fly-ash based "geopolymers"," *Applied Geochemistry*, vol. 19, no. 3, pp. 423–434, 2004.

[9] L. Zheng, W. Wang, and Y. Shi, "The effects of alkaline dosage and Si/Al ratio on the immobilization of heavy metals in municipal solid waste incineration fly ash-based geopolymer," *Chemosphere*, vol. 79, no. 6, pp. 665–671, 2010.

[10] J. Zhang, J. L. Provis, D. Feng, and J. S. J. van Deventer, "Geopolymers for immobilization of Cr^{6+}, Cd^{2+} and Pb^{2+}," *Journal of Hazardous Materials*, vol. 157, no. 2-3, pp. 587–598, 2008.

[11] J. Deja, "Immobilization of Cr^{6+}, Cd^{2+}, Zn^{2+} and Pb^{2+} in alkali-activated slag binders," *Cement and Concrete Research*, vol. 32, no. 12, pp. 1971–1979, 2002.

[12] J. G. S. van Jaarsveld and J. S. J. van Deventer, "The effect of metal contaminants on the formation and properties of waste-based geopolymers," *Cement and Concrete Research*, vol. 29, no. 8, pp. 1189–1200, 1999.

[13] L. Kalina, J. Koplík, F. Šoukal, J. Másilko, and L. Jaskowiecová, "Potential uses of geopolymers to immobilize toxic metals from by-products material," *Environmental Engineering and Management Journal*, vol. 11, no. 3, pp. 579–584, 2012.

[14] J. Koplík, L. Kalina, J. Másilko, and F. Šoukal, "The characterization of fixation of Ba, Pb, and Cu in alkali-activated fly ash/blast furnace slag matrix," *Materials*, vol. 9, no. 7, p. 533, 2016.